ISSN 1070-3284, Russian Journal of Coordination Chemistry, 2019, Vol. 45, No. 5, pp. 309–319. © Pleiades Publishing, Ltd., 2019.
Russian Text © The Author(s), 2019, published in Koordinatsionnaya Khimiya, 2019, Vol. 45, No. 5, pp. 259–269.

Bis-*o*-Semiquinonate Zinc Complexes with the Bidentate N-Donor Ligands: Synthesis and Magnetic Properties

A. V. Piskunov[a], *, A. V. Maleeva[a], A. S. Bogomyakov[b], and G. K. Fukin[a]

[a] *Razuvaev Institute of Organometallic Chemistry, Russian Academy of Sciences, Nizhny Novgorod, 603600 Russia*

[b] *International Tomography Center, Siberian Branch, Russian Academy of Sciences, Novosibirsk, 630090 Russia*

**e-mail: pial@iomc.ras.ru*

Received June 26, 2018; revised November 8, 2018; accepted December 3, 2018

Abstract—Biradical mononuclear $SQ_2ZnL^4_2$ and SQ_2ZnL^5 complexes, binuclear $SQ_2Zn(L^3)ZnSQ_2$ complex, and coordination polymers $(SQ_2ZnL^{1(2)})_n$ are synthesized by the reactions of bis(3,6-di-*tert*-butyl-*o*-benzosemiquinonato)zinc (SQ_2Zn) with the bidentate N-donor ligands ($L^{1–5}$) (pyrazine (L^1), 4,4'-dipyridyl (L^2), phenazine (L^3), 4-cyanopyridine (L^4), and pyrimidine (L^5)). The structures of the synthesized compounds are determined by X-ray diffraction analysis (CIF files CCDC nos. 1846558–1846563). The binuclear $SQ_2Zn(L^3)ZnSQ_2$ and mononuclear SQ_2ZnL^5 complexes contain pentacoordinated metal atoms, whereas zinc in the compounds based on the $L^{1,2,4}$ ligands exists in the octahedral environment with the *trans*-arranged *o*-semiquinonate ligands. The coordination polymers $(SQ_2ZnL^{1(2)})_n$ are capable of depolymerizing on dissolution in organic solvents. According to the data of measuring the temperature dependence of the magnetic susceptibility, the antiferromagnetic exchange between unpaired electrons of the organic radical anions is observed in crystals of the synthesized compounds.

Keywords: *o*-semiquinone ligands, zinc, X-ray diffraction analysis, magnetochemical studies

DOI: 10.1134/S1070328419050026

INTRODUCTION

The studies of the molecular and electronic structures of the metal complexes with the redox-active ligands represent a very promising and intensively developed trend of the modern coordination and organoelement chemistry. An important aspect should be distinguished among the variety of significant chemical and physicochemical properties of the compounds of this type, namely, their magnetic activity and the possibility of controlling it in wide ranges by the variation of the nature of the complexing metals and paramagnetic ligands. This fact enables one to consider the metal complexes with the redox-active ligands as potential building blocks for manufacturing magnetic materials [1–3]. It should be mentioned that the formation of the stable organometallic coordination polymer [4] completely satisfies the requirements imposed on functional materials. The first successful attempts to prepare coordination polymers containing the paramagnetic *o*-semiquinone ligands were made for the cobalt [5] and manganese complexes [6] in which the $(dioxolene)_2M$ moieties were linked by pyrazine into polymer chains. Later diverse structures where metal bis-*o*-semiquinolates were synthesized were bound into polymer chains by various dipyridyl linkers. The copper compounds [7], redox-isomeric cobalt derivatives [8–13], and catalytically active manganese complexes [14, 15] were obtained. The first polymer zinc bis-*o*-benzosemiquinonate was prepared as a result of studying the possibilities of the mechanochemical synthesis of the metal bis-*o*-semiquinolates [16].

In terms of the present work, we attempted to synthesize coordination polymers based on the bis(3,6-di-*tert*-butyl-*o*-benzosemiquinonato)zinc biradical moiety and some bidentate N-donor ligands.

EXPERIMENTAL

All procedures on the syntheses of the zinc complexes were carried out under anaerobic conditions. The solvents used were purified and dehydrated according to published recommendations [17]. The following commercial reagents were used: pyrazine (L^1), 4,4'-dipyridyl (L^2), phenazine (L^3), 4-cyanopyridine (L^4), and pyrimidine (L^5). The initial zinc complex $SQ_2Zn(Et_2O)_2$ (SQ_2Zn is bis(3,6-di-*tert*-butyl-*o*-benzosemiquinonato)zinc) was synthesized using a known procedure [18].

Synthesis of complexes I–IV. A solution of a necessary amount of the neutral N-donor ligand in toluene (10 mL) was poured to a solution of the zinc complex

$SQ_2Zn(Et_2O)_2$ (0.5 mmol) in toluene (15 mL). The obtained reaction mixture was heated in a water bath for 30 min, after which the liquid phase was removed under reduced pressure. The dark blue residue was recrystallized from an appropriate solvent.

Complex SQ_2ZnL^1 (I): (a) $m(L^1)$ = 0.04 g. The crystals of $SQ_2ZnL^1 \cdot C_7H_8$ (**Ia**) suitable for X-ray diffraction analysis (XRD) were obtained by the slow cooling of the toluene solution. The yield was 0.27 g (79%).

IR (Nujol), ν, cm^{-1}: 451 s, 501 s, 553 m, 655 s, 674 s, 702 w, 798 w, 804 m, 829 s, 930 w, 957 s, 1027 w, 1044 m, 1053 s, 1073 w, 1107 w, 1129 m, 1153 m, 1180 m, 1202 m, 1234 w, 1276 s, 1344 s, 1363 m, 1386 w, 1419 s, 1456 w, 1504 w, 1551 w, 1568 w, 1614 w.

For $C_{39}H_{52}N_2O_4Zn$

Anal. calcd., %	C, 69.07	H, 7.73	N, 4.13
Found, %	C, 69.25	H, 7.89	N, 3.96

(b) $m(L^1)$ = 0.04 g. The crystals of $SQ_2ZnL^1 \cdot C_6H_{14}$ (**Ib**) suitable for XRD were obtained from a CH_2Cl_2–hexane (1 : 1) mixture. The yield was 0.23 g (68%).

IR (Nujol), ν, cm^{-1}: 451 s, 501 s, 553 m, 655 s, 674 s, 702 w, 798 w, 804 m, 829 s, 930 w, 957 s, 1027 w, 1044 m, 1053 s, 1073 w, 1107 w, 1129 m, 1153 m, 1180 m, 1202 m, 1234 w, 1276 s, 1344 s, 1363 m, 1386 w, 1419 s, 1456 w, 1504 w, 1551 w, 1568 w, 1614 w.

For $C_{38}H_{58}N_2O_4Zn$

Anal. calcd., %	C, 67.89	H, 8.70	N, 4.17
Found, %	C, 68.23	H, 8.98	N, 4.05

Complex SQ_2ZnL^2 (II): (a) $m(L^2)$ = 0.079 g. The crystals of **II** · $3C_7H_8$ suitable for XRD were obtained by the slow cooling of the toluene solution. The yield was 0.38 g (82%).

IR (Nujol), ν, cm^{-1}: 462 w, 499 m, 528 w, 625 s, 651 s, 665 m, 677 w, 697 w, 810 s, 821 s, 831 w, 852 w, 926 w, 948 s, 974 w, 988 w, 1005 w, 1024 w, 1041 w, 1062 m, 1111 w, 1126 w, 1176 m, 1203 w, 1216 m, 1276 m, 1319 w, 1342 m, 1352 m, 1360 m, 1405 s, 1438 s, 1478 s, 1537 m, 1601 s.

For $C_{59}H_{72}N_2O_4Zn$

Anal. calcd., %	C, 75.50	H, 7.73	N, 2.98
Found, %	C, 75.68	H, 7.82	N, 2.77

Complex $SQ_2Zn(L^3)ZnSQ_2$ (III): (a) $m(L^3)$ = 0.045 g. The crystals of **III** · $4C_7H_8$ suitable for XRD were obtained by the slow cooling of the toluene solution. The yield was 0.28 g (72%).

IR (Nujol), ν, cm^{-1}: 463 w, 503 m, 554 m, 594 m, 654 s, 661 w, 675 s, 702 w, 728 w, 746 s, 805 w, 823 w, 834 w, 919 w, 956 s, 965 w, 1026 w, 1058 m, 1129 m, 1182 w, 1204 m, 1237 w, 1278 w, 1289 w, 1311 w, 1344 m, 1356 m, 1386 m, 1454 s, 1488 s, 1504 s, 1521 w, 1557 w, 1610 w.

For $C_{96}H_{120}N_2O_8Zn_2$

Anal. calcd., %	C, 73.88	H, 7.75	N, 1.79
Found, %	C, 74.12	H, 7.91	N, 1.57

Complex $SQ_2ZnL^4_2$ (IV): (a) $m(L^4)$ = 0.104 g. The crystals of **IV** suitable for XRD were obtained by the slow cooling of the toluene solution. The yield was 0.23 g (65%).

IR (Nujol), ν, cm^{-1}: 463 w, 503 m, 537 m, 563 s, 601 w, 655 s, 674 m, 692 w, 705 w, 729 m, 753 w, 776 w, 801 w, 829 s, 866 w, 926 w, 955 s, 979 w, 1016 m, 1027 m, 1071 w, 1092 w, 1110 m, 1182 m, 1200 m, 1205 m, 1218 m, 1276 s, 1318 w, 1327 w, 1342 m, 1351 m, 1358 m, 1416 m, 1553 s, 1605 s, 2242 m.

For $C_{40}H_{48}N_4O_4Zn$

Anal. calcd., %	C, 67.27	H, 6.77	N, 7.84
Found, %	C, 67.45	H, 6.89	N, 7.72

Complex SQ_2ZnL^5 (V): (a) $m(L^5)$ = 0.04 g. The crystals of **V** suitable for XRD were obtained by the slow cooling of the toluene solution. The yield was 0.17 g (58%).

IR (Nujol), ν, cm^{-1}: 462 w, 499 m, 553 m, 598 w, 636 m, 655 s, 675 m, 692 w, 712 m, 727 m, 804 w, 814 w, 831 m, 890 w, 927 w, 954 s, 1011 m, 1026 m, 1048 w, 1080 m, 1167 m, 1180 m, 1199 w, 1205 w, 1228 w, 1238 w, 1279 m, 1344 m, 1351 m, 1364 m, 1385 s, 1408 s, 1477 s, 1490 s, 1550 w, 1564 w, 1589 s.

For $C_{32}H_{44}N_2O_4Zn$

Anal. calcd., %	C, 65.58	H, 7.57	N, 4.78
Found, %	C, 65.73	H, 7.68	N, 4.59

IR spectra were recorded on an FSM-1201 FTIR spectrometer in Nujol in KBr cells. EPR spectra were detected on a Bruker EMX spectrometer. 2,2-Diphenyl-1-picrylhydrazyl (g = 2.0037) served as a standard for the determination of the g factor. In order to determine the precise parameters, the EPR spectrum was simulated using the WinEPR SimFonia program (Bruker).

The magnetic susceptibility of polycrystalline samples of the complexes was measured on a Quantum Design MPMSXL SQUID magnetometer in the temperature range from 2 to 300 K in a magnetic field of 0.5 T. In the calculations of the paramagnetic component of the magnetic susceptibility (χ) of the complexes, the additive diamagnetic contribution of ions was taken into account according to Pascal's con-

stants. The effective magnetic moments at various temperatures were calculated by the equation

$$\mu_{eff}(T) = \left(\frac{3k}{N\beta^2}\chi T\right)^{1/2} \approx (8\chi T)^{1/2},$$

where N, k, and β are Avogadro's number, the Boltzmann constant, and the Bohr magneton, respectively.

XRD analyses of the complexes were carried out on Smart Apex I (**Ia**, **III**). Bruker D8 Quest (**Ib**, **V**), and Oxford Xcalibur (**II**, **IV**) diffractometers at 100 K ($\lambda(MoK_\alpha)$ = 0.71073 Å). The structures of the compounds were determined by direct methods and refined by least squares for F^2 in the full-matrix anisotropic approximation for all non-hydrogen atoms (SHELXTL) [19]. An absorption correction was applied using the SADABS [20] (**Ia**, **Ib**, **III**, and **V**) and ABSPACK [21] (**II** and **IV**) programs. Selected bond lengths and bond angles in the molecules of compounds **I**–**V** are presented in Table 1. The crystallographic parameters and the structure refinement details are given in Table 2.

The crystallographic data were deposited with the Cambridge Crystallographic Data Centre (CIF files CCDC nos. 1846558–1846563); deposit@ccdc.cam.ac.uk; http://www.ccdc.cam.ac.uk).

RESULTS AND DISCUSSION

The standard ligand exchange procedure successfully used previously for the design of the magnesium [22, 23] and zinc bis-*o*-semiquinone complexes [24–26] was applied to obtain a series of the complexes. A solution of the neutral ligand L^1, L^2, L^3, L^4, or L^5 in toluene was poured to a solution of SQ_2Zn bearing two molecules of coordinated diethyl ether in the same solvent (Scheme 1). The reactions of formation of complexes **I**, **III**, **IV**, and **V** are insensitive to the stoichiometry of the initial reagents. Regardless of the ratio of SQ_2Zn to the neutral ligand L^1 (L^3, L^4, or L^5) (2 : 1, 1 : 1, or 1 : 2), coordination polymer **I**, binuclear complex **III**, and mononuclear complexes **IV** and **V** were isolated in the crystalline state. The reaction with 4,4'-dipyridyl at the 1 : 1 reagent ratio makes it possible to obtain coordination polymer **II** presented in Scheme 1. The binuclear complex published earlier is formed in a deficient of the nitrogen-containing ligand [26].

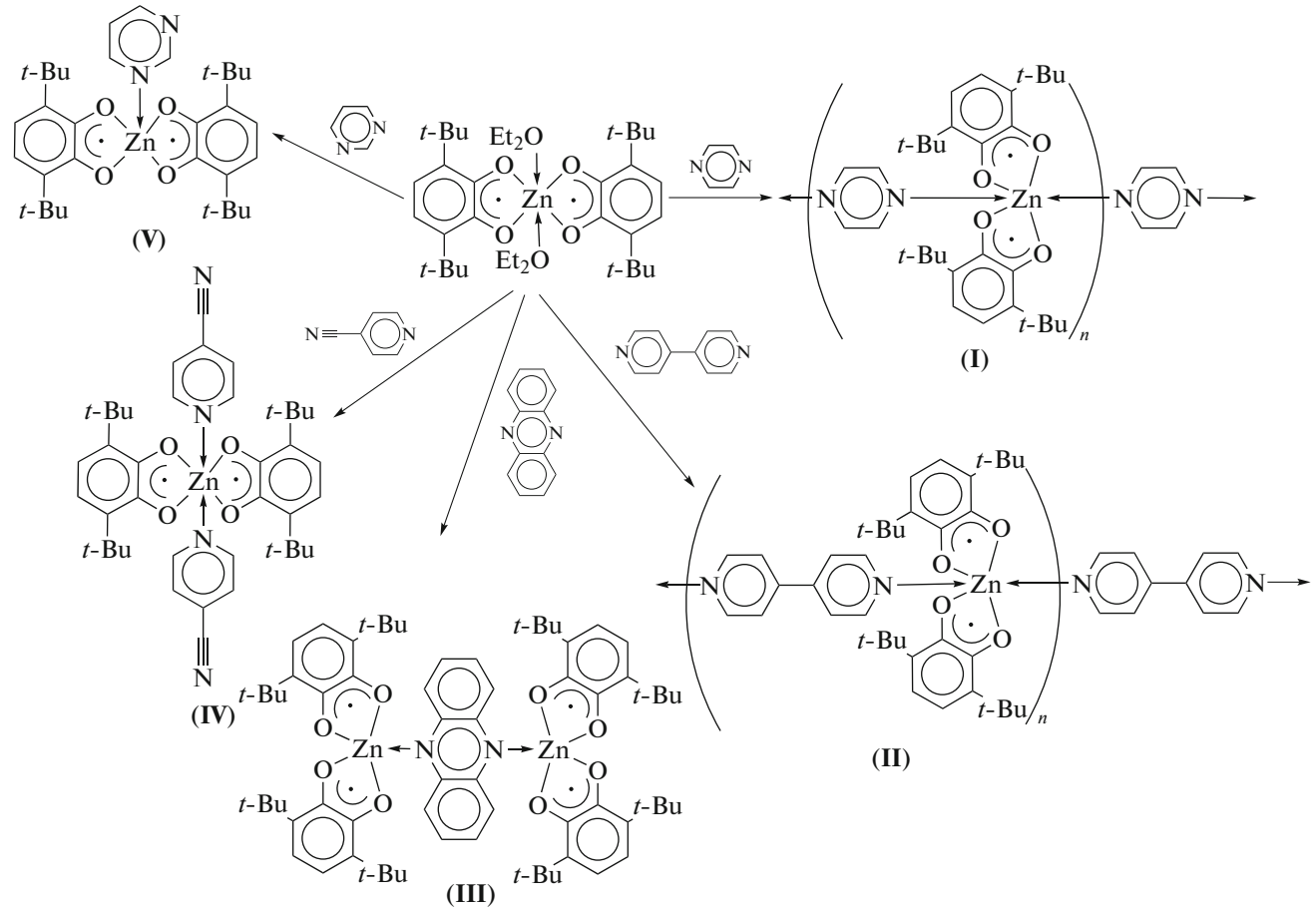

Scheme 1.

Table 1. Selected bond lengths (Å) and bond angles (deg) in complexes **I–V**

Bond	**Ia**	**Ib**	**II**	**III**	**IV**	**V**
Zn(1)–O(1)	2.058(3)	2.0421(10)	2.0670(10)	2.0398(17)	2.0306(12)	2.017(6)
Zn(1)–O(2)	2.039(3)	2.0379(10)	2.0713(11)	2.0225(17)		2.017(6)
Zn(1)–O(3)	2.052(3)		2.0826(10)	2.0140(17)		
Zn(1)–O(4)	2.054(3)		2.0827(10)	2.0282(17)		
Zn(1)–N(1)	2.213(3)	2.2798(16)	2.1272(13)	2.102(2)	2.243(3)	2.130(6)
Zn(1)–N(2)	2.189(3)	2.2109(16)	2.2635(13)			
O(1)–C(1)	1.287(5)	1.2787(17)	1.2763(18)	1.283(3)	1.276(2)	1.316(7)
O(2)–C(2)	1.279(4)	1.2819(15)	1.2797(18)	1.285(3)		1.316(7)
O(3)–C(7)	1.295(4)		1.2750(18)			
O(4)–C(8)	1.283(5)		1.2841(18)			
C(1)–C(2)	1.475(6)	1.476(2)	1.488(2)	1.480(3)	1.440(2)	1.480(4)
C(1)–C(1*A*)					1.472(3)	
C(1)–C(6)	1.455(5)	1.4426(18)	1.444(2)	1.436(3)		1.428(4)
C(2)–C(3)	1.444(6)	1.437(2)	1.440(2)	1.433(3)	1.370(2)	1.425(4)
C(3)–C(4)	1.370(5)	1.3716(19)	1.373(2)	1.367(3)		1.365(4)
C(3)–C(3*A*)					1.422(3)	
C(4)–C(5)	1.407(6)	1.420(2)	1.421(2)	1.425(3)		1.425(4)
C(5)–C(6)	1.369(6)	1.362(2)	1.373(2)	1.370(3)		1.364(4)
C(7)–C(8)	1.460(6)		1.484(2)			
C(8)–C(9)	1.462(6)		1.440(2)			
C(9)–C(10)	1.372(6)		1.369(2)			
C(10)–C(11)	1.403(6)		1.533(2)			
C(11)–C(12)	1.371(6)		1.424(2)			
C(7)–C(12)	1.449(6)		1.444(2)			
Angle	**Ia**	**Ib**	**II**	**III**	**IV**	**V**
O(1)Zn(1)O(2)	80.86(11)	80.80(4)	79.19(4)	80.24(7)		81.3(2)
O(1)Zn(1)O(4)	97.67(11)		172.72(4)	148.49(7)		
O(1)Zn(1)O(1*A*)		174.10(6)			99.50(7)	140.20(12)
O(1)Zn(1)O(1*B*)					180.00(10)	
O(1)Zn(1)O(3)	177.52(13)		100.70(4)	89.11(7)		
O(1)Zn(1)O(2*A*)		99.12(4)				90.5(2)
O(2)Zn(1)O(4)	178.02(12)		99.58(4)	91.85(7)		
O(2)Zn(1)O(1*A*)						
O(2)Zn(1)O(3)	100.44(11)		171.85(4)	146.22(7)		
O(2)Zn(1)O(2*A*)		178.36(6)				140.15(12)
O(1*A*)Zn(1)O(3)	80.98(11)		79.48(4)			
O(1*A*)Zn(1)O(2*A*)						
O(1)Zn(1)N(1)	87.93(13)	87.05(3)	92.43(5)	102.41(7)	98.59(5)	95.1(3)
O(2)Zn(1)N(1)	90.61(13)	89.18(3)	94.85(5)	105.99(7)		107.6(3)
O(4)Zn(1)N(1)	87.29(12)		93.66(5)	109.08(7)		
O(1*A*)Zn(1)N(1)					81.41(5)	
O(2*A*)Zn(1)N(1)	89.92(13)					
O(3)Zn(1)N(1)			94.47(4)	107.60(7)		
O(1)Zn(1)N(2)	90.61(13)	92.95(3)	85.64(4)			
O(2)Zn(1)N(2)	92.11(13)	90.82(3)	87.09(4)			
O(4)Zn(1)N(2)	89.23(13)		86.02(4)			
O(1*A*)Zn(1)N(2)						
O(3)Zn(1)N(2)	91.46(13)		85.87(4)			
O(2*A*)Zn(1)N(2)						
N(1)Zn(1)N(2)	176.02(14)	180.0	178.06(5)			

Table 2. Crystallographic data and XRD parameters for compounds **I–V**

Parameter	Value					
	Ia	**Ib**	**II**	**III**	**IV**	**V**
FW	678.19	672.23	938.55	1560.67	714.19	586.06
Crystal system	Tetragonal	Monoclinic	Triclinic	Triclinic	Tetragonal	Monoclinic
Space group	$P4_12_12$	$P2_1/c$	$P\bar{1}$	$P\bar{1}$	$P4_2/mnm$	$P2_1/n$
a, Å	14.342(2)	28.5467(8)	11.45372(13)	11.0257(14)	10.29120(10)	10.2662(3)
b, Å	14.342(2)	7.2684(2)	12.91641(18)	12.3052(18)	10.29120(10)	10.2695(3)
c, Å	37.188(6)	19.6044(5)	19.6170(3)	17.128(3)	17.8078(2)	17.6397(5)
α, deg	90	90	103.3422(12)	72.662(2)	90	90
β, deg	90	110.7250(10)	99.2711(11)	73.001(3)	90	90.0260(10)
γ, deg	90	90	103.0182(11)	79.257(2)	90	90
V, Å^3	7650(3)	3804.47(18)	2680.85(6)	2108.8(5)	1886.00	1859.73(9)
Z	8	4	2	1	2	2
ρ, g/cm^3	1.178	1.174	1.163	1.229	1.258	1.047
μ, mm^{-1}	0.681	0.684	0.504	0.626	0.695	0.691
Crystal size, mm	0.390 × 0.350 × 0.090	0.360 × 0.120 × 0.100	0.500 × 0.400 × 0.300	0.300 × 0.120 × 0.060	0.300 × 0.150 × 0.100	0.430 × 0.300 × 0.260
θ_{min}–θ_{max}, deg	2.008–26.998	2.221–27.999	2.996–26.000	1.880–29.000	3.024–26.976	3.044–25.996
Total number of reflections	32115	38934	38937	22342	29124	37006
Independent reflections	8183	4554	10479	11053	1148	3596
R_{int}	0.0687	0.0273	0.0316	0.0571	0.0365	0.0319
Reflections with $I > 2\sigma(I)$	6443	4320	9381	7468	1070	3255
Number of refined parameters	470	249	610	501	101	228
R ($I > 2\sigma(I)$)	$R_1 = 0.0517$ $wR_2 = 0.0961$	$R_1 = 0.0322$ $wR_2 = 0.0797$	$R_1 = 0.0339$ $wR_2 = 0.0806$	$R_1 = 0.0591$ $wR_2 = 0.1032$	$R_1 = 0.0266$ $wR_2 = 0.0658$	$R_1 = 0.0829$ $wR_2 = 0.2270$
GOOF (F^2)	1.025	1.066	1.037	1.023	1.076	1.066
$\Delta\rho_{max}/\Delta_{min}$, e Å^{-3}	0.618/–0.292	0.529/–0.595	0.477/–0.318	0.847/–0.555	0.336–0.306	1.329–0.975

In the case of complex **I**, two polymorphous forms were obtained by crystallization from different solvents. The crystals of compound **Ia** of the first type were obtained by the slow cooling of a toluene solution, and the second type crystals (**Ib**) were obtained by the addition of hexane to a solution of SQ_2ZnL^1 in dichloromethane. The crystal unit cells of complexes **Ia** and **Ib** contain molecules of solvate solvents (one molecule of toluene or hexane, respectively, per complex molecule). The crystals of compound **II** suitable for XRD were obtained by the slow cooling of the SQ_2ZnL^2 complex in toluene solution. The crystal unit cell of complex **II** contains three solvate molecules of toluene. Complexes **Ia**, **Ib**, and **II** are coordination polymers, but their crystal packings differ crucially. The chains of the $(SQ_2ZnL)_n$ coordination polymer are perpendicular to each other in the crystal of complex **Ia**, while only parallel chains are observed in the crystals of complexes **Ib** and **II**. The metal atoms in the molecules of complexes **Ia**, **Ib**, and **II** exist in distorted octahedral environments (Fig. 1). The equatorial plane in the octahedron is occupied by the oxygen atoms of the dioxolene ligands, and the nitrogen atoms of the N-donor ligands are located in the axial positions. The *o*-semiquinone ligands in the crystals of compounds **I** and **II** are somewhat convex to one of the nitrogen bridging ligands. The dihedral angle between the planes of the *o*-semiquinone ligands is 9.94°, 15.63°, and 42.28° for complexes **Ia**, **Ib**, and **II**, respectively. This arrangement results in the nonequivalent binding of zinc to nitrogen. The longer bond of zinc with nitrogen is observed with the pyrazine (dipyridyl) moiety toward which the bending occurs (Zn–N(2) for the crystals of complex **Ia** (**Ib**) and Zn–N(1) in the case of complex **II**) (Fig. 1). The aromatic rings of the dipyridyl ligand in the polymer chains of compound **II** are noncoplanar, and the dihedral angle between their planes is 49.79°. The N(1)Zn(1)N(2) angle is 176.02°, 180°, and 178.06° in complexes **Ia**, **Ib**, and **II**, respectively.

The bridging bidentate N-donor ligand in complex **III** is phenazine inducing an enhanced steric hindrance of the coordination center compared to analogous pyrazine. This situation results in a significantly larger bending angle along the SQ–Zn–SQ line, and the dihedral angle between the *o*-semiquinone ligands increases over that in compound **I** and is equal to 54.49°. As a result, no polymer structure is observed in a molecule of compound **III**. The compound represents a binuclear complex in which phenazine binds two pentacoordinate metal centers (Fig. 2). The zinc atoms in compound **III** are characterized by the tetragonal pyramidal coordination mode, the oxygen atoms of the *o*-semiquinone ligands form the pyramid base, and the nitrogen atoms of phenazine are in the apical positions. The crystal unit cell of complex **III** also contains four molecules of solvate toluene.

The cyano groups of the 4-cyanopyridine ligand in complex **IV** are not involved in coordination bonds. Regardless of the ratio of the initial reagents, the compound containing two molecules of the neutral ligand and the hexacoordinate metal atom is formed during the formation of the crystalline phase (Fig. 2). On the one hand, the pentacoordinate metal derivatives have previously been synthesized by the reactions of bis(3,6-di-*tert*-butyl-*o*-benzosemiquinolato)zinc with 4-imino-substituted pyridines [26]. On the other hand, the data on the complex formation of SQ_2Zn with 4-cyanopyridine are consistent with the results obtained by the studies of the related cobalt [27] and manganese compounds [28]. The crystal unit cell of compound **IV** contains three solvate molecules of toluene per molecule of the complex. 4-Cyanopyridine is disordered over two positions due to which the zinc atom lies on two mutually perpendicular 2-fold axes. As for compounds **I** and **II**, the base of the octahedral coordination polyhedron is formed by the oxygen atoms of the *o*-semiquinone ligands and the nitrogen atoms occupy the apical positions. The Zn(1)–N(1) bond is not orthogonal to the equatorial plane. The nitrogen atom deviates from the rigidly vertical position by 13.37°.

The ratio $SQ_2Zn : L^5 = 1 : 1$ is observed in complex **V**. However, the second nitrogen atom is not coordinated to the metal atom of the adjacent molecules, which does not allow the coordination polymer to be formed. The aromatic systems of the *o*-semiquinone ligands are parallel and lie in one plane (Fig. 2). The zinc atom is disordered over two positions arranged above and under this plane at a distance of 0.734 Å. The plane of the Zn(1)O(1)C(1)C(2)O(2) chelate cycle forms the dihedral angle equal to 15.78° with the plane of aromatic systems of the *o*-semiquinone ligands. The pyrimidine moiety in the molecule of compound **V** is disordered over four positions.

The Zn–O and Zn–N distances in complexes **I**–**V** lie in the ranges characteristic of compounds this type with five- and pentacoordinate metal atoms [16, 18, 24–26]. The metal–oxygen and metal–nitrogen distances increase regularly on going from pentacoordinate complexes **III** and **V** to hexacoordinate complexes **I**, **II**, and **IV**. The C–O bond lengths and the C–C bond length distribution in the diolate ligand are typical of the *o*-semiquinolate ligands and confirm its radical anion character. The quinoid alternation of bonds is observed in the aromatic ring of the radical anion ligand [29, 30].

All synthesized complexes **I**–**V** are deeply blue, resistant to air moisture and oxygen (in the crystalline state), and moderately soluble in organic solvents. The polycrystalline samples of compounds **I**–**V** demonstrate a broad unresolved EPR spectrum at both room temperature and 77 K with the *g* factor equal to 2.002, which is typical of organic free radicals. The EPR spectra of complexes **I**–**V** in the frozen toluene matrix

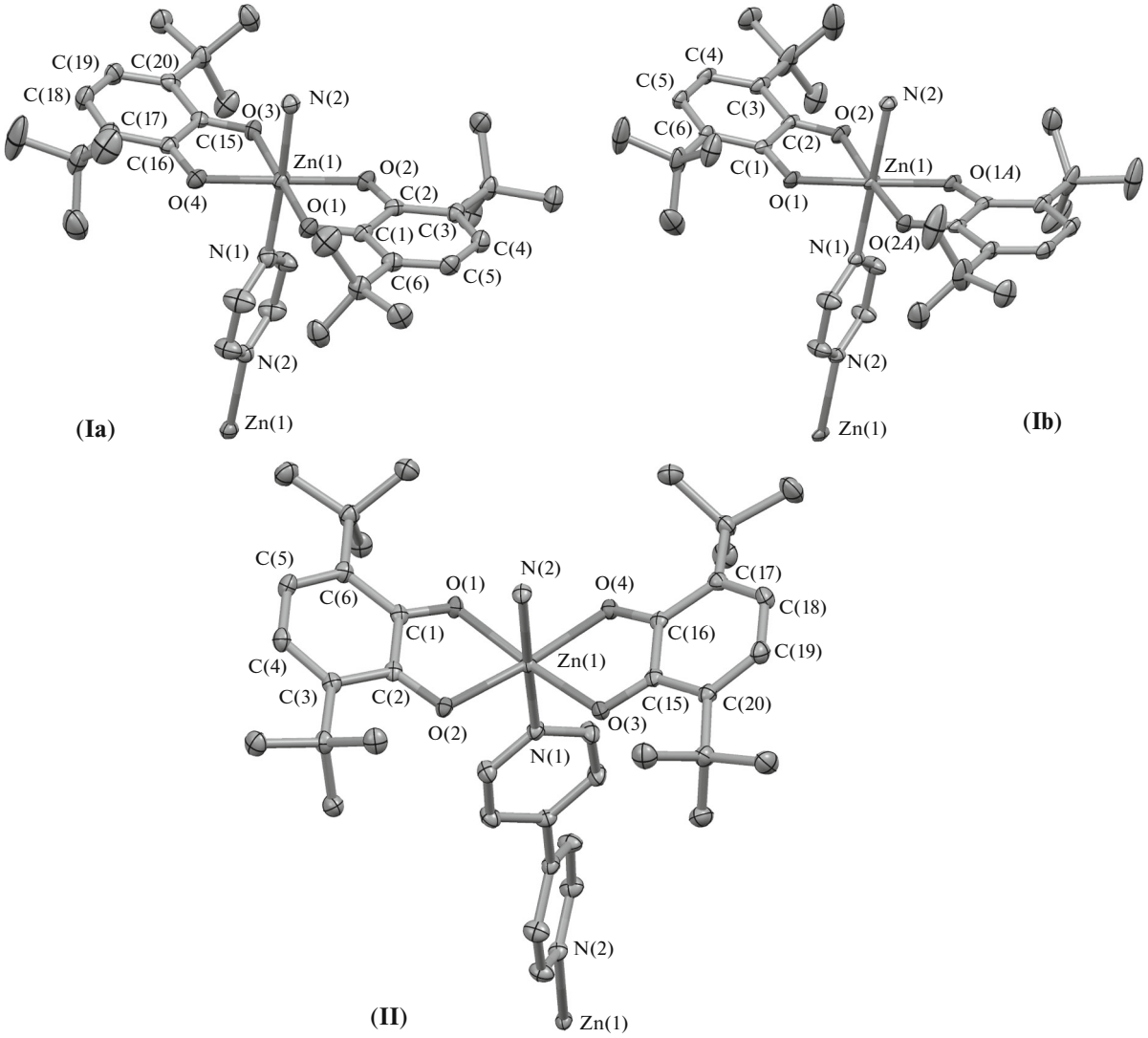

Fig. 1. Molecular structures of the monomeric units in coordination polymers **Ia**, **Ib**, and **II**. Thermal ellipsoids of 50% probability are presented. Hydrogen atoms are omitted for clarity.

demonstrate a superposition of signals of several types. All compounds are characterized by well resolved singlets at $g = 4$ characteristic of biradical species and attributed to the forbidden transition $\Delta m_s = 2$. The superposition of the singlet responsible for the monoradical impurity formed upon the dissociation (association) of zinc bis-*o*-semiquinolates in a solution and the signal characterizing the dipole–dipole interaction in biradical systems is observed at $g = 2$ (Fig. 3). For the precise determination of the splitting parameters of complexes **I**–**V** in the zero field, their EPR spectra recorded at 150 K were simulated using the WinEPR Simfonia software package. The zero-field splitting parameters of the EPR spectra of biradical complexes **I**–**V** are presented in Table 3. It should be mentioned that the spectral parameters for complexes **I** and **II** are close to those observed for similar pentacoordinate compounds [18, 26]. This fact together with a good solubility of the coordination polymers indicates the cleavage of the longer Zn–N bond in the polymer chain. The cleavage of one of the Zn–N coordination bonds is also indicated by the EPR spectrum of hexacoordinate complex **IV** exhibiting signals from two different biradical species. The predominant signal with the parameter $|D| = 179$ G (0.0167 cm^{-1}) corresponds to the initial hexacoordinate complex, whereas the second signal (minor, $|D| =$ 204 G (0.0191 cm^{-1})) corresponds to the dissociation product with the elimination of one of the cyanopyridyl ligands to form the corresponding pentacoordinate derivative.

The temperature dependences of the effective magnetic moment (μ_{eff}) for complexes **I**–**V** are presented in Fig. 4. The high-temperature values of μ_{eff} for compounds **Ia**, **Ib**, **II**, **IV**, and **V** (2.40, 2.43, 2.44, 2.45, and

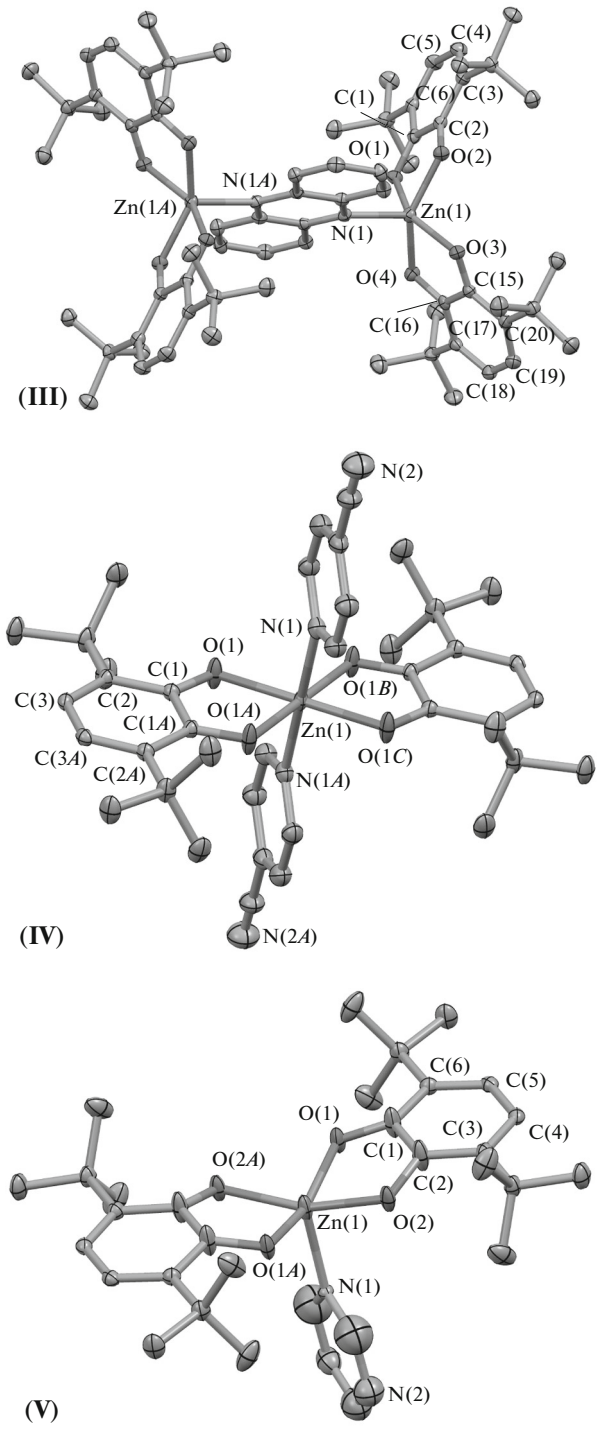

Fig. 2. Molecular structures of complexes **III**, **IV**, and **V**. Thermal ellipsoids of 50% probability are presented. Hydrogen atoms are omitted for clarity.

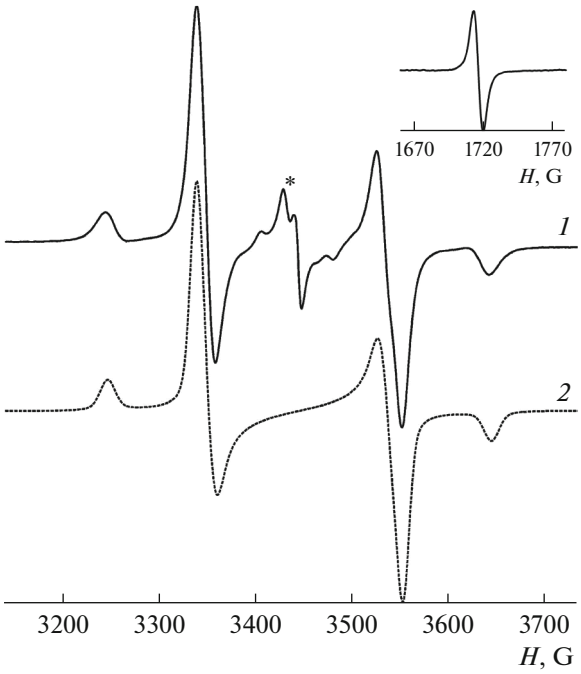

Fig. 3. (*1*) Experimental and (*2*) simulated EPR spectra of complex **I** in the frozen toluene matrix (150 K). The signal from the monoradical impurity in the experimental spectrum is designated by *. The signal corresponding to the forbidden transition $\Delta m_s = 2$ is presented in inset. Simulation parameters: $S = 1$, $|D| = 199$ G, $|E| = 5$ G, $g_X = 2.0023$, $g_Y = 2.0010$, $g_Z = 2.0020$, $\Delta H_X = 15$ G, $\Delta H_Y = 12$ G, $\Delta H_Z = 15$ G, and $L/G = 0.2$.

2.20 μ_B, respectively, at $T = 300$ K) are close to the theoretical spin-only value (2.45 μ_B) for two noninteracting SQ ligands with spins $S = 1/2$ at the g factor equal to 2. The calculation for the coordination polymers was based on one monomer unit. For binuclear complex **III**, the value of μ_{eff} (3.11 μ_B at $T = 300$ K) corresponds to the theoretical spin-only value equal to 3.46 μ_B for four noninteracting SQ ligands with spins $S = 1/2$ at a g factor of 2 (Fig. 4). For all compounds, the values of μ_{eff} decrease smoothly followed by the temperature decrease down to 50 K. The values of μ_{eff} noticeably decrease below 50 K and reach values close to 0 μ_B at 5 K. This behavior of the $\mu_{eff}(T)$ dependences indicates antiferromagnetic exchange interactions between spins of the SQ ligands. The exchange interaction parameters in the complexes were estimated in terms of the exchange-coupled dimer model ($H = -2JS_1S_2$). The calculated exchange interaction parameters are presented in Table 4. The use of the exchange-coupled dimer model for the $(SQ)_2Zn$ moieties in coordination polymers **Ia** and **Ib** allows one to estimate the exchange parameter only, because the value obtained for interdimeric interactions (-25 cm^{-1}) is approximately comparable with the exchange inside the $\{(SQ)_2Zn\}$ moiety. The high parameter of intercluster exchange interactions indicates that comparable exchange interactions are observed both in the $\{(SQ)_2Zn\}$ moieties and between them. However, no appropriate analytical expressions are available at the moment for such models of exchange-coupled chains.

Table 3. Splitting parameters in the zero field of the EPR spectra of biradical complexes **I**–**V** in the frozen toluene matrix at $T = 150$ K

Complex	$\|D\|$, G/cm^{-1}	$\|E\|$, G/cm^{-1}	r, Å*
I	199/0.0186	5/0.0005	5.42
II	200/0.0187	6/0.0006	5.41
III	205/0.0191	7/0.0006	5.37
IV	204/0.0190	5/0.0005	5.38
	179/0.0167	7/0.0006	5.59
V	206/0.0192	6/0.0006	5.36

***** The distance between the radical centers calculated in the approximation of the point dipole interaction [37].

Table 4. Optimum values of the g factor, exchange interaction parameters J and zJ', and the monomer impurity p for complexes **I**–**V** according to the magnetochemical data

Complex	g	J, cm^{-1}	zJ', cm^{-1}	p, %
Ia	2.07	–17.5	–24.1	3.6
Ib	2.0 (fix.)	–32.5	–10	5
II	1.98	–12.3	0	0
III	2.09	–94.6	0	0.5
IV	2.04	–20.3	0	0.3
V	1.90	–45.0	0	0.4

The exchange interaction changes from ferromagnetic to antiferromagnetic and the exchange energy increases by the absolute value on going from the previously published hexacoordinate bis-*o*-semiquinone zinc complexes with the *cis*-arranged radical ligands [25] to their nearest analogs with the *trans*-arranged diolate fragments (complexes **I**, **II**, and **IV**). In addition, an increase in the exchange energy is also favored by the distortion of the octahedral coordination environment (complex **IV**) toward the tetragonal bipyramidal one with the elongation of one of the Zn–N bonds (compounds **I** and **II**). The direct magnetic exchange between the radical ligands was proposed [26] as the main chanel determining the magnetic behavior of pentacoordinate zinc bis-*o*-semiquinolates. The dependence of the exchange energy on the distance between the centers of spin density delocalization in the organic ligands was found. The data obtained in this work are well consistent with the results obtained previously for similar biradical zinc compounds **VI**–**IX** [18, 26] (Scheme 2).

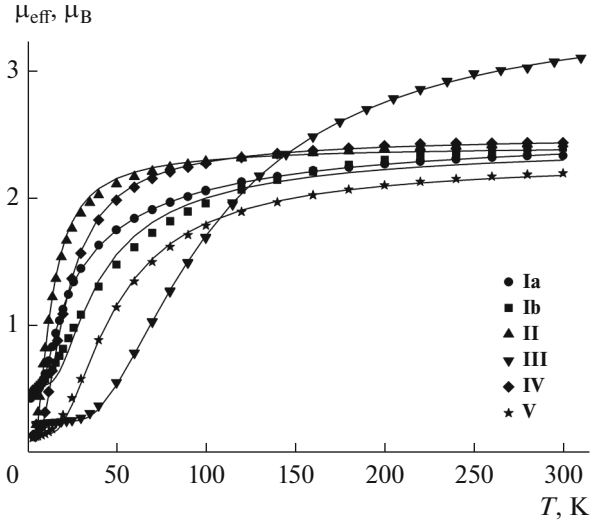

Fig. 4. (Signs) experimental and (lines) theoretical $\mu_{eff}(T)$ dependences for complexes **I**–**V**.

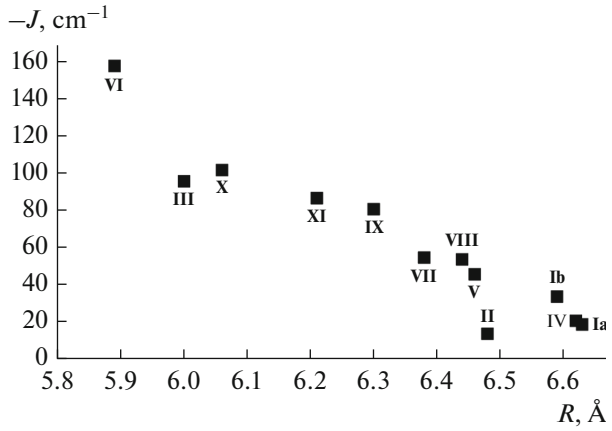

Fig. 5. Energy of the antiferromagnetic exchange vs. distance between the radical centers in biradical complexes **I**–**XI**.

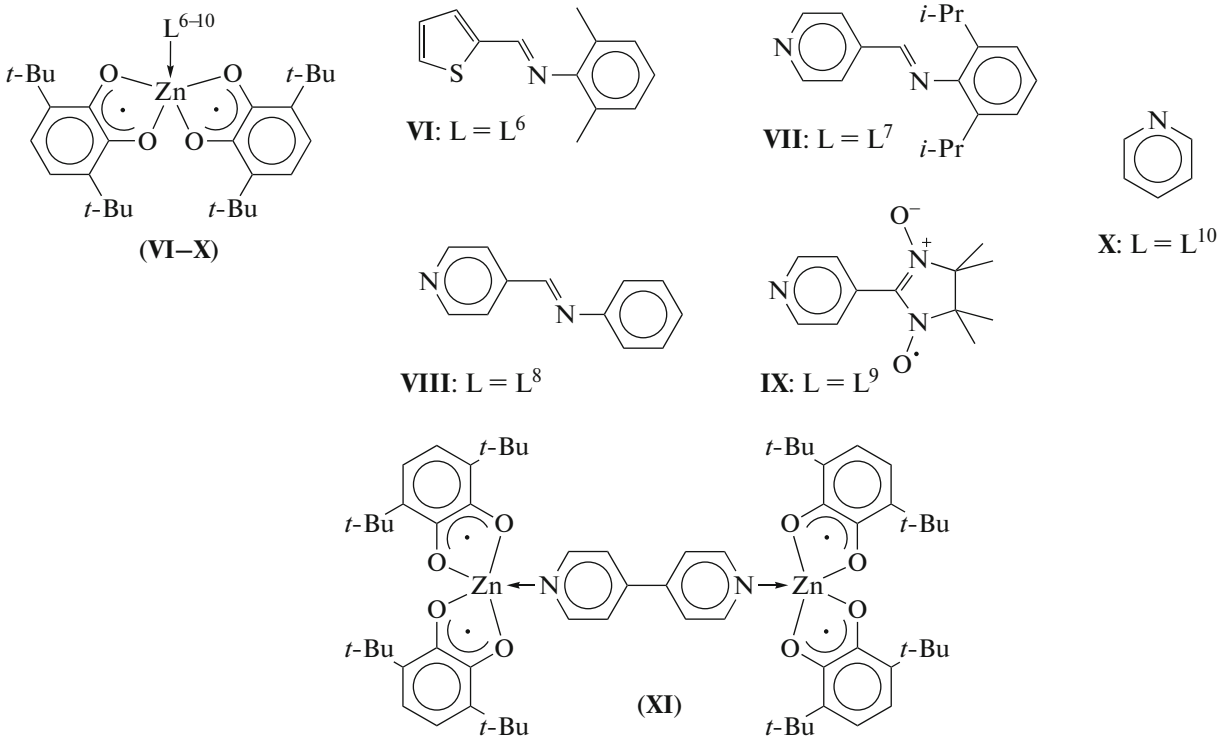

Scheme 2.

The dependence $-J = f(R)$, where R is the distance between the radicals determined as a separation between the centroids built with the C(1–6), O(1), O(2) and C(15–20), O(3), O(4) atoms, is presented in Fig. 5. The results obtained for complexes **I**–**V** in this study were combined with the recently published results [26] for compounds **VI**–**IX**. The correspondence of the presented results suggests that the channel of the direct magnetic exchange also predominates in the case of compounds **I**–**V**. It is important that the indirect exchange channel prevails for the related biradical complexes of trivalent elements (Al, Ga, and In) containing the valence-bonded diamagnetic anion as an apical substituent rather than a neutral donor ligand [31–36]. The indirect exchange channel is related to the overlapping of the magnetic orbitals of the organic ligands with the σ*-M–X bond (M = Ga, Al; X is anionic apical substituent) [31, 32] or to the inclusion of lone electron pairs of heteroatoms X into the formation of semioccupied orbitals [35].

To conclude, the new mono-, binuclear and polymer zinc bis-*o*-semiquinone complexes containing various bridging bidentate N-donor ligands were synthesized in this work. The molecular structures of the synthesized complexes were determined by XRD. The coordination polymer bearing the pyrazine bridge forms two polymorphous crystalline modifications differed in the mutual arrangement of the polymer chains. All compounds studied are characterized by the antiferromagnetic interaction between odd electrons of the organic paramagnetic ligands.

ACKNOWLEDGMENTS

The physicochemical studies of the compounds were carried out using the equipment of the Analytical Center of the Razuvaev Institute of Organometallic Chemistry (Russian Academy of Sciences).

FUNDING

This work was supported by the Russian Science Foundation, project no. 14-13-01296.

REFERENCES

1. Ovcharenko, V.I. and Sagdeev, R.Z., *Russ. Chem. Rev.*, 1999, vol. 68, p. 345.
2. Koivisto, B.D. and Hicks, R.G., *Coord. Chem. Rev.*, 2005, vol. 249, p. 2612.
3. Ratera, I. and Veciana, J., *Chem. Soc. Rev.*, 2012, vol. 41, p. 303.
4. D'Alessandro, D.M., *Chem. Commun.*, 2016, vol. 52, p. 8957.
5. Jung, O.-S. and Pierpont, C.G., *J. Am. Chem. Soc.*, 1994, vol. 116, p. 2229.
6. Attia, A.S. and Pierpont, C.G., *Inorg. Chem.*, 1997, vol. 36, p. 6184.
7. Abakumov, G.A., Lobanov, A.V., Cherkasov, V.K., et al., *Dokl. Akad. Nauk SSSR*, 1985, vol. 285, p. 906.
8. Chen, X.-Y., Wei, R.-J., Zheng, L.-S., and Tao, J., *Inorg. Chem.*, 2014, vol. 53, p. 13212.
9. Chen, L., Wei, R., Tao, J., et al., *Sci. China Chem.*, 2012, vol. 55, p. 1037.

10. Imaz, I., Maspoch, D., Rodriguez-Blanco, C., et al., *Angew. Chem., Int. Ed.*, 2008, vol. 47, p. 1857.
11. Drath, O., Gable, R.W., Poneti, G., et al., *Cryst. Growth Des.*, 2017, vol. 17, p. 3156.
12. Drath, O., Gable, R.W., Moubaraki, B., et al., *Inorg. Chem.*, 2016, vol. 55, p. 4141.
13. Cheng, W.-Q., Li, G.-L., Zhang, R., et al., *J. Mol. Struct.*, 2015, vol. 1087, p. 68.
14. Goswami, S., Panja, A., Butcher, R.J., et al., *Inorg. Chim. Acta*, 2011, vol. 370, p. 311.
15. Shaikh, N., Goswami, S., Panja, A., et al., *Inorg. Chem.*, 2005, vol. 44, p. 9714.
16. Glavinovic, M., Qi, F., Katsenis, A.D., et al., *Chem. Sci.*, 2016, vol. 7, p. 707.
17. Gordon, A. and Ford, R., *The Chemist's Companion: A Handbook of Practical Data, Techniques, and References*, New York: Wiley, 1972.
18. Piskunov, A.V., Maleeva, A.V., Abakumov, G.A., et al., *Russ. J. Coord. Chem.*, 2011, vol. 37, p. 243. doi 10.1134/S1070328411030092
19. Sheldrick, G.M., *SHELXTL. Version 6.12. Structure Determination Software Suite*, Madison: Bruker AXS, 2000.
20. Sheldrick, G.M., *SADABS. Version 2.01. Bruker/Siemens Area Detector Absorption Correction Program*, Madison: Bruker AXS, 1998.
21. Agilent Technologies. CrysAlis Pro, Yarnton: Agilent Technologies Ltd., 2011.
22. Piskunov, A.V, Lado, A.V., Abakumov, G.A. et al., *Russ. Chem. Bull.*, 2007, vol. 56, p. 97. doi 10.1007/s11172-007-0016-1
23. Piskunov, A.V., Maleeva, A.V., Bogomyakov, A.S., and Fukin, G.K., *Russ. Chem. Bull.*, 2017, vol. 66, p. 1618. doi 10.1007/s11172-017-1933-2
24. Ilyakina, E.V., Poddel'sky, A.I., Piskunov, A.V., et al., *New J. Chem.*, 2012, vol. 36, p. 1944.
25. Piskunov, A.V., Maleeva, A.V., Bogomyakov, A.S., et al., *Polyhedron*, 2015, vol. 102, p. 715.
26. Piskunov, A.V., Maleeva, A.V., Fukin, G.K., et al., *Inorg. Chim. Acta*, 2017, vol. 455, p. 213.
27. Schmidt, R.D., Shultz, D.A., Martin, J.D., and Boyle, P.D., *J. Am. Chem. Soc.*, 2010, vol. 132, p. 6261.
28. Jana, N.Ch., Brandao, P., and Panja, P., *J. Inorg. Biochem.*, 2016, vol. 159, p. 96.
29. Poddels'ky, A.I., Cherkasov, V.K., and Abakumov, G.A., *Coord. Chem. Rev.*, 2009, vol. 253, p. 291.
30. Brown, S.N., *Inorg. Chem.*, 2012, vol. 51, p. 1251.
31. Myers, T.W., Holmes, A.L., and Berben, L.A., *Inorg. Chem.*, 2012, vol. 51, p. 8997.
32. Cates, C.D., Myers, T.W., and Berben, L.A., *Inorg. Chem.*, 2012, vol. 51, p. 11891.
33. Piskunov, A.V., Mescheryakova, I.N., Bogomyakov, A.S., et al., *Inorg. Chem. Commun.*, 2009, vol. 12, p. 1067.
34. Piskunov, A.V., Meshcheryakova, I.N., Ershova, I.V., et al., *RSC Adv.*, 2014, vol. 4, p. 42494.
35. Piskunov, A.V., Ershova, I.V., Bogomyakov, A.S., et al., *Inorg. Chem.*, 2015, vol. 54, p. 6090.
36. Piskunov, A.V., Ershova, I.V., Bogomyakov, A.S., et al., *Inorg. Chem. Commun.*, 2016, vol. 66, p. 94.
37. Carrington, A. and McLachlan, A., *Introduction to Magnetic Resonance with Application to Chemistry and Chemical Physics*, New Yoork: Harper & Row, 1967.

Translated by E. Yablonskaya